Annex C: Simulated Changes in Vegetation Distribution under Global Warming

C.1. Introduction

Global vegetation models (GVM) have in the past decade evolved from largely statistical-correlational to more process-based, rendering greater confidence in their abilities to address questions of global change. There are generally two classes of GVMs, biogeography models and biogeochemistry models. The biogeography models place emphasis on determination of what can live where, but either do not calculate or only partially calculate the cycling of carbon and nutrients within ecosystems. The biogeochemistry models simulate the carbon and nutrient cycles within ecosystems, but lack the ability to determine what kind of vegetation could live at a given location. BIOME3 has significantly blurred this model distinction (Haxeltine and Prentice, 1996). There are over 20 biogeochemistry models and about 5 biogeography models. Two of the biogeography models, MAPSS (Neilson, 1995) and BIOME3 were used to provide estimates of changes in vegetation distribution, density and hydrology for this IPCC special report. These are equilibrium models, which simulate the potential 'climax' vegetation that could live at any well-drained, upland site in the world under an 'average' seasonal climate. Equilibrium models provide useful 'snapshots' of what a terrestrial biosphere in equilibrium with its climate might look like, but can provide only inferential information about how the biosphere will make transitions from one condition to another. This is in contrast to other models, which simulate the timeseries of vegetation change at a point (Shugart and Smith, 1996), but which do not produce maps of vegetation distribution and function. Fully dynamic versions of the spatially-explicit GVMs are being developed and incorporate both biogeography and biogeochemistry processes, but the dynamic global vegetation models (DGVM) are not yet ready for assessment purposes (Neilson and Running, 1996). Several model intercomparison projects are underway and can serve to provide some context for the two models used here. One such intercomparison is the VEMAP process.

C.2. VEMAP Model Intercomparison

The Vegetation/Ecosystem Modeling and Analysis Project (VEMAP) compared three biogeography models, MAPSS (Neilson, 1995), BIOME2 (Haxeltine et al., 1996), and DOLY (Woodward and Smith, 1994; Woodward et al., 1995) and three biogeochemistry models TEM (Raich et al., 1991; McGuire et al., 1992; Melillo et al., 1993), CENTURY (Parton et al., 1987; Parton et al., 1988; Parton et al., 1993), and BIOME-BGC (Hunt and Running, 1992; Running and Hunt, 1993). The two classes of global models were intercompared and loosely coupled for an assessment of both model capabilities and the potential impacts of global warming on U.S. ecosystems (VEMAP Members, 1995). The VEMAP process determined that all the models have roughly equal skill in simulating the current environment, but exhibit some divergences under alternative climates, in some cases producing vegetation responses of opposite sign.

Given the timeframe of this IPCC special report, only MAPSS and BIOME3 were able to provide global simulations. MAPSS and BIOME2 (a precursor to BIOME3) were found to produce generally similar results under the future climate scenarios of the VEMAP process. However, MAPSS is consistently more sensitive to water stress, producing a more xeric outcome under future climates and it also has a more sensitive response to elevated CO_2. That is, when incorporating a direct, physiological CO_2 effect, MAPSS produces a larger benefit to vegetation from increased water-use-efficiency (VEMAP Members, 1995).

C.3. Biogeography Model Description

MAPSS (Mapped Atmosphere-Plant-Soil System; Neilson, 1995) and BIOME3 (Haxeltine and Prentice,

1996) are among a new generation of process-based, equilibrium biogeographic models (IPCC 1996, WG II, Section 1.3.4; VEMAP Members, 1995). The models simulate the distribution of potential global vegetation based on local vegetation and hydrologic processes and the physiological properties of plants. Both models simulate the mixture of vegetation lifeforms, such as trees, shrubs, and grasses, that can coexist at a site while in competition with each other for light and water. A set of physiologically-grounded 'rules' determines whether the woody vegetation will be broadleaved or needleleaved, or evergreen or deciduous, as well as other properties. The models also simulate the maximum carrying capacity, or vegetation density, in the form of leaf area that can be supported at the site, under the constraints of energy and water. Energy constraints, largely applicable to cold ecosystems, are prescribed in MAPSS, but are simulated by an explicit carbon flux model in BIOME3. The two models simulate a similar set of water balance processes, incorporating soil texture effects.

Thus, MAPSS and BIOME3 simulate the distribution of vegetation, such as forests, savannas, shrubland, grasslands and deserts over all non-wetland sites of the Earth, based on the relative densities or productivity of overstory and understory, vegetation leaf characteristics and thermal tolerances. The models simulate the distribution of generalized vegetation lifeforms (e.g. tree, shrub, grass; evergreen-deciduous; broadleaf-needleleaf), rather than species and assemble these into a vegetation type classification. There are currently 45 different vegetation types simulated by MAPSS and 18 by BIOME3. The vegetation types are hierarchical, representing biomes (e.g., boreal forest, temperate savanna, grassland, etc.) at the top and more detailed community-level descriptions at the lower end (e.g., subtropical, xeromorphic woodland). Only the top of the hierarchy is utilized in this analysis. Since both models simulate a full site water balance, they are also calibrated and tested hydrologic models, thereby, allowing estimates of impacts on water resources fully integrated with the simulated impacts on vegetation (Neilson and Marks, 1994; VEMAP Members, 1995). As equilibrium models, MAPSS and BIOME3 simulate vegetation distribution and hydrology under an average seasonal cycle of climate. They simulate an equilibrium land-surface biosphere under current or future climate, but not the transitional vegetation changes from one climate to another. Thus, the models show the long term potential consequences of climate change, but one can only infer immediate (1-10 year) effects.

MAPSS and BIOME3 contain algorithms that allow the incorporation of a direct physiological CO_2 effect. Elevated CO_2 concentrations can, among other effects, enhance productivity and increase the water-use-efficiency (WUE, carbon fixed per unit water transpired) of the vegetation thereby reducing the sensitivity of the vegetation to drought stress (IPCC 1996, WG II, Section A.2.3; Bazzaz et al., 1996; Eamus, 1991). BIOME3 allows a direct CO_2 effect on both productivity and water-use-efficiency. MAPSS accomplishes the same effect by reducing stomatal conductance, which then results in increased leaf area, thus indirectly incorporating a productivity effect. Individual species exhibit variations in their expressions of direct CO_2 effects. For example, the productivity and WUE effects are not necessarily tightly coupled (Eamus, 1996a). However, since the models simulate functional types, rather than species, both models have generalized the direct CO_2 effects to all vegetation, with the exception in BIOME3 of differentiating C_3 and C_4 physiological types. In BIOME3 C_4 plants do not experience the elevated growth of C_3 plants, but do experience increased water-use-efficiency. The realized importance of the direct CO_2 processes in complex, mature ecosystems remains a matter of debate (Bazzaz et al., 1996).

A review of 58 studies indicated an average 32% increase in plant dry mass under a doubling of CO_2 concentration (Wullschleger, Post, and King, 1995). Norby (1996) documented an average 29% increase in annual growth per unit leaf area in seven broadleaf tree species under 2 x CO_2 over a wide range of conditions. Increased WUE, examined in another review, averaged about 30-40% as indexed by reductions in leaf conductance to water vapor (Eamus, 1991). If such responses were maintained in forests over many decades, they would imply a substantial potential for increased storage of atmospheric carbon, as well as conferring some increased tolerance to drought due to increased WUE. However, some species or ecosystems exhibit acclimation to elevated CO_2 by downregulating photosynthesis

(Bazzaz, 1990; Grulke et al., 1993; Grulke et al., 1990); while others do not exhibit acclimation (Bazzaz, 1990; Teskey, 1997). Most of the early CO_2 research was done on juvenile trees in pots and growth chambers. New research is beginning to emerge which focuses on larger trees or intact forested ecosystems. Recent reviews of this newer literature (Eamus, 1996a; Curtis, 1996) indicate that acclimation may not be as prevalent when roots are unconstrained and also that leaf conductance may not be reduced and that both responses are dependent on the experimental conditions, the length of exposure and the degree of nutrient or water stress. These results imply that forests could produce more leaf area under elevated CO_2, but may not gain a benefit from increased WUE. In fact, with increased leaf area, transpiration should increase on a per tree basis and the stand would use more water. Elevated temperatures would increase transpiration even further, perhaps drying the soils and inducing a drought effect on the ecosystem (ibid). Prominent among the environmental influences that are thought to moderate long-term responses to elevated CO_2 is nitrogen supply (Kirschbaum et al., 1994; McGuire et al., 1995; Eamus, 1996b). Unless CO_2 stimulates an increase in N mineralization (Curtis et al., 1995), productivity gains in high CO_2 are likely to be constrained by the system's N budget (Körner, 1995). Nitrogen limitations may constrain carbon gains to structural tissue, rather than leaves (Curtis et al., 1995). Thus, in areas receiving large amounts of N deposition, a direct CO_2 response could result in large increases in leaf area, increasing transpiration and possibly increasing sensitivity to drought via rapid soil water depletion. Early growth increases may disappear as the system approaches carrying capacity as limited by water or nutrients (Körner, 1995). Shifts in species composition will likely result from different sensitivities to elevated CO_2 (Bazzaz et al., 1996; Körner, 1995). Both MAPSS and BIOME3 have been operated with and without the direct CO_2 effects in this study in order to gauge the importance and sensitivity of the processes within the modeling framework. The direct effects of elevated CO_2 are imparted only in the ecological model processes and not in the GCMs. There are no feedbacks between the ecological and atmospheric models

The MAPSS model also contains a fire model that shifts some vegetation to a 'fire climax' state, such as in many grasslands or savannas. BIOME3 embeds these processes in the calibration. Neither model considers current or past land-use practices. Thus, some areas that the models indicate as grassland, for example, might actually be shrublands, due to either grazing or fire suppression. Although the two models do not simulate actual land-use, the 'potential' land-cover simulated by the models should provide an accurate estimate of the land-surface potential. That is, forests cannot be grown in deserts or shrublands without irrigation; and, agricultural productivity should be higher in a potential forest landscape than in a potential shrubland landscape (given similar soils). Changes in LAI can be interpreted as a change in the overall carrying capacity or standing crop of the site, regardless of whether it is in potential natural vegetation or under cultivation. Additions from irrigation or nitrogen could alter this conclusion, but it should hold for non-irrigated, upland systems. Thus, simulated changes in potential natural vegetation should be valuable indicators of general shifts in agricultural potential.

C.4. Vegetation Classification

The vegetation classification from each model has been aggregated to ten broad classes for MAPSS and nine for BIOME3. The models are most accurate in differentiating the broad physiognomic divisions of Forest, Savanna, semi-arid lands (Shrublands and Grasslands) and Arid Lands. These differences are largely based on the relationship between leaf area and site water balance and the simulated changes in leaf area and site water balance should be generally reliable (especially with respect to the sign of the change). The aggregated vegetation classes used for this analysis are as follows.

1. *Tundra* is defined as the treeless vegetation which extends beyond treeline at high latitudes and altitudes, regardless of whether it is dominated by dwarf shrubs or herbaceous plants.
2. *Taiga/Tundra* is the broad 'ecotonal' region of open woodland, which occurs at higher latitudes or elevations beyond the 'closed' Boreal forest. This type is not explicitly simulated by BIOME3, but rather is included in Boreal Conifer Forest.
3. *Boreal Conifer Forest* is the Taiga proper, i.e., relatively dense forest composed mainly of needle-leaved trees and occurring in cold-winter climates.
4. *Temperate Evergreen Forest* encompasses the wet temperate and subtropical conifer forests of the NorthWest in North America, as well as subtropical evergreen broadleaf forests (e.g., in China) and the Nothofagus and Eucalyptus forests of the Southern Hemisphere.
5. *Temperate Mixed Forest* includes pure temperate broadleaf forests, such as oak-hickory, or beech-maple. It also includes mixtures of broadleaf and temperate evergreen types, such as the cool-mixed pine/fir and hardwood forests of the northeastern United States or the warm-mixed pine/hardwood forests of the southeastern U.S.
6. *Tropical Broadleaf Forest* includes both tropical evergreen forest and dense tropical drought-deciduous forests.
7. *Savanna/Woodlands* encompass all 'open' tree vegetation from high to low latitudes and elevations. The tropical dry savannas and drought deciduous forests are contained within this class. So too are the temperate pine savannas and 'pygmy' forests and the aspen woodlands adjacent to the boreal forest. Fire can play an important role in maintaining the open nature of these woodlands; while, grazing can increase the density of woody vegetation at the expense of grass.
8. *Shrub/Woodlands* are distinguished from the Savanna/Woodlands by their lower biomass and shorter stature. This is a drier vegetation type than the Savanna/Woodlands and encompasses most semi-arid vegetation types from Chaparral to mesquite woodlands to cold, semi-desert sage shrublands. The actual vegetation associated with this type is very susceptible to variation depending on soils, topography, fire, grazing and land-use history. Distinctions between shrub-steppe and grassland are sometimes difficult to quantify, given that each usually contains elements of both grass and woody vegetation. The relative abundance of the two functional types is considered in determining the classification, but there are no generally accepted rules to indicate how much woody vegetation is sufficient to label a region a shrubland, or conversely how much grass is required to label it a grassland.
9. *Grasslands* include both C_3 and C_4 grassland types in both temperate and tropical regions. Much of the grassland type is a 'fire climax' type that would be populated by shrubs either with the absence of fire, or with extensive grazing.
10. *Arid Lands* encompass all regions drier than grasslands, from hyper-arid to semi-arid, ranging from the "waterless" deserts such as the Namib to the 'semi-deserts' of central Asia and Patagonia. The regions could be more or less 'grassy' or 'shrubby' depending on disturbance and land-use history.

C.5. Future Climate Scenarios

Estimation of the potential impacts of global warming should utilize several future climate scenarios, since the magnitude, timing and spatial details of global warming vary among climate models. Most published impacts studies were based on atmospheric General Circulation Model (GCM) doubled CO_2 radiative forcing equilibrium experiments with simple mixed-layer oceans. Doubled CO_2 radiative forcing (2 x CO_2) includes only about 50% actual CO_2 forcing with the balance arising from other greenhouse gases. More recent, transient experiments with coupled atmosphere-ocean GCMs have suggested a global average increase in temperature of about 1.0-3.5°C by the time of CO_2 doubling, estimated as 60-70 years from now (described in the IPCC Second Assessment Report, SAR; IPCC 1996, WG I, Section 6; Annex B). The most recent GCMs include sulfate aerosols in some experiments, which can cool the climate. The analysis presented here will rely both on the older 2 x CO_2 equilibrium GCM scenarios (described in the IPCC First Assessment Report, FAR; IPCC 1990, WG I, Section 3; Annex B), since most published analyses have relied on them, and on three new simulations, two from the Hadley Center (HADCM2GHG and HADCM2SUL; Johns et al., submitted; Mitchell et al., 1995; IPCC 1996, WG I, Sections 5, 6), and one from the Max Planck Institute for Meteorology (MPI-T106; Bengtsson, et al. 1995; Bengtsson, et al., 1996; IPCC 1996, WG I, Section 6), which have been made using coupled atmosphere-ocean GCMs and considering sulfate aerosol forcing.

To allow direct comparison with the previously completed VEMAP simulations over the conterminous U.S. (VEMAP Members, 1995), the same three equilibrium GCM scenarios were utilized for the global simulations: UKMO (Mitchell and Warrilow, 1987); GFDL-R30 (IPCC 1990, WG I, Section 3; IPCC 1990, WG I, Section 5); and OSU (Schlesinger and Zhao, 1989). The coarse grid from each model was interpolated to a 0.5° x 0.5°, lat.-long. grid. Scenarios were constructed by applying ratios ((2 x CO_2)/(1 x CO_2)) of all climate variables (except temperature) back to a baseline longterm average monthly climate dataset (Leemans and Cramer, 1991). Ratios were used to avoid negative numbers (e.g., negative precipitation), but were not allowed to exceed 5, to prevent unrealistic changes in regions with normally low rainfall. Temperature scenarios were calculated as a difference ((2 x CO_2) - (1 x CO_2)) and applied to the baseline dataset.

The newer GCM scenarios are extracted from transient GCM simulations wherein trace gases were allowed to increase gradually over a long period of years, allowing the climate to adjust while incorporating inherent lags in the ocean-atmosphere systems. In order to run the equilibrium vegetation models under the newer transient GCMs, a control climate is extracted as an average of either 30 years (Hadley Center) or 10 years (Max Planck Institute) of model output associated with present climate (e.g. 1961-1990). Likewise, a 30 or 10 year average is extracted from the time period approximating 2 x CO_2 forcing (e.g. 2070- 2099). These average climates are then used to drive the vegetation models. Note that because the vegetation models are equilibrium models, the results must be interpreted as indicating the potential vegetation, i.e., the climatically suitable vegetation. Time lags and transient responses of the vegetation to climate change are not considered here.

C.6. Interpretation of Biogeographic Model Simulations

Each of the ten IPCC regions was supplied with a set of MAPSS and BIOME3 output. Included were figures of vegetation distribution under current and future climate, vegetation density change (indexed by leaf area change), and runoff change. Also included were summary tables of the areas of the different biomes within each region under current and future climate, a change matrix indicating the area shifts

from current biome type to other types, the areas within each biome expected to undergo an increase or decrease in vegetation density (change in LAI) and the areas within each biome expected to undergo an increase or decrease in annual runoff. These results were supplied for each vegetation model and for each GCM scenario. MAPSS and BIOME3 were both run under the Hadley Center scenarios; BIOME3 alone was run under the Max Planck Institute scenario; and, MAPSS alone was run under the older OSU, GFDL-R30 and UKMO scenarios. The Hadley and MPI simulations were run both with and without a direct CO_2 effect (applied in the ecological models); while, the OSU, GFDL-R30 and UKMO scenarios were only run with the direct CO_2 effects incorporated, in keeping with the VEMAP analyses.

Since the regional maps are of a much smaller extent and include quantitative information, the detailed interpretation will be left to the regions and the following discussion will only address general features of the simulations, particularly the differences between the older and newer GCMs and the MAPSS and BIOME3 intercomparisons. Although each region received the full set of figures, only a subset will be presented here. The MAPSS and BIOME3 results are sufficiently similar that the ranges presented in Tables C-1, C-2, C-3, C-4 and C-5 encompass the output from both models to indicate the full range of uncertainties within the scope of these experiments and models.

Table C-1: Potential future biome area (percentage of current) simulated by the MAPSS and BIOME3 biogeography models under three older (IPCC 1990, WG I), equilibrium 2 x CO_2 GCM scenarios and under three newer (IPCC 1996, WG I), transient simulations from which 2 x CO_2 scenarios were extracted. The reported ranges include both ecological models under several GCM scenarios. The baseline areas estimates are outputs from each model. Since BIOME3 does not differentiate Taiga/Tundra from Boreal Forest, two different aggregations are presented. The Taiga/Tundra summaries are MAPSS data only; while the "Boreal + Taiga/Tundra" and "Total Forest + Taiga/Tundra" summaries are from both models. The ranges of percent change for Boreal Conifer are from both models (except FAR scenarios, which are MAPSS output). The Taiga/Tundra under the MAPSS simulations decreases in area in all scenarios; while, Boreal conifer increases in area. Were these two vegetation zones aggregated in MAPSS, they would exhibit either increases or decreases, as in the BIOME3 simulations. The decreases in Boreal Conifer, shown in the table, are BIOME3 simulations.

Biome Type	Baseline Area (Mha)		With CO_2 Effect		Without CO_2 Effect
	MAPSS	BIOME3	FAR Scenarios	SAR Scenarios	SAR Scenarios
Tundra	792	950	33-59%	43-60%	43-60%
Taiga/Tundra	999		35-62%	56-64%	56-64%
Boreal Conifer Forest	1,024	1,992	109-133%	64-116%	68-111%
Boreal + Taiga/Tundra	2,023	1,992	72-95%	64-90%	68-87%
Temperate Evergreen Forest	1,142	816	104-121%	104-137%	84-109%

Temperate Mixed Forest	744	1,192	125-161%	139-199%	104-162%
Total Temperate Forest	1,886	2,008	116-125%	137-158%	107-131%
Tropical Broadleaf Forest	1,406	1,582	71-151%	120-138%	70-108%
Savanna/Woodland	2,698	2,942	90-130%	78-89%	100-115%
Shrub-Steppe	994	1,954	61-70%	70-136%	81-123%
Grassland	2,082	554	109-126%	45-123%	120-136%
Total Shrub/Grassland	3,076	2,508	96-108%	105-127%	111-126%
Arid Lands	1,470	1,351	71-72%	59-78%	83-120%
Total Vegetation	13,351	13,333	100-101%	100-101%	100-101%

Note: FAR = First Assessment Report (IPCC 1990, WG I); SAR = Second Assessment Report (IPCC 1996, WG I).

Table C-2: Percentage area of current biomes which could undergo a loss of leaf area (i.e., biomass decrease) due to global warming under various older (FAR) and newer (SAR) GCM scenarios, and with or without a direct CO_2 effect (see Table C-1 for details), as simulated by the MAPSS and BIOME3 biogeography models (ranges include both models). The losses in leaf area generally indicate a less favorable water balance (drought).

	With CO_2 Effect		Without CO_2 Effect
Biome Type	FAR Scenarios	SAR Scenarios	SAR Scenarios
Tundra	1-3%	0-1%	0-2%
Taiga/Tundra	1-5%	1%	2%
Boreal Conifer Forests	39-67%	0-20%	3-69%
Temperate Evergreen Forests	24-57%	1-18%	28-51%
Temperate Mixed Forests	54-86%	1-29%	15-75%
Tropical Broadleaf Forests	5-63%	1-42%	26-33%
Savanna/Woodlands	10-21%	7-17%	38-75%
Shrub-Steppe	26-45%	1-24%	20-59%

Grasslands	33-37%	5-46%	43-75%
Arid Lands	8-12%	0-13%	0-29%

Table C-3: Percentage area of current biomes which could undergo a gain of leaf area (i.e., biomass increase) due to global warming under various older (FAR) and newer (SAR) GCM scenarios, and with or without a direct CO_2 effect (see Table C-1 for details), as simulated by the MAPSS and BIOME3 biogeography models (ranges include both models). The gains in leaf area generally indicate a more favorable water balance.

Biome Type	With CO_2 Effect		Without CO_2 Effect
	FAR Scenarios	SAR Scenarios	SAR Scenarios
Tundra	20-74%	20-58%	49-82%
Taiga/Tundra	91-98%	92-95%	91-94%
Boreal Conifer Forests	13-21%	36-93%	3-58%
Temperate Evergreen Forests	20-41%	46-67%	7-18%
Temperate Mixed Forests	4-26%	50-91%	9-21%
Tropical Broadleaf Forests	7-40%	16-87%	0-7%
Savanna/Woodlands	74-88%	46-84%	4-31%
Shrub-Steppe	46-64%	64-80%	16-42%
Grasslands	56-60%	45-78%	3-28%
Arid Lands	51-57%	53-80%	23-66%

Table C-4: Percentage area of current biomes which could undergo a loss of annual runoff due to global warming under various older (FAR) and newer (SAR) GCM scenarios, and with or without a direct CO_2 effect (see Table C-1 for details), as simulated by the MAPSS and BIOME3 biogeography models (ranges include both models).

Biome Type	With CO_2 Effect		Without CO_2 Effect
	FAR Scenarios	SAR Scenarios	SAR Scenarios

Tundra	19-32%	16-45%	28-46%
Taiga/Tundra	79-90%	71-79%	76-82%
Boreal Conifer Forests	1-25%	3-53%	33-81%
Temperate Evergreen Forests	12-21%	25-37%	33-67%
Temperate Mixed Forests	59-77%	51-66%	62-68%
Tropical Broadleaf Forests	11-40%	15-54%	23-68%
Savanna/Woodlands	14-19%	37-60%	31-46%
Shrub-Steppe	43-61%	23-44%	18-42%
Grasslands	34-38%	41-60%	33-56%
Arid Lands	24-26%	1-20%	2-20%

Table C-5: Percentage area of current biomes which could undergo a gain of annual runoff due to global warming under various older (FAR) and newer (SAR) GCM scenarios, and with or without a direct CO_2 effect (see Table C-1 for details), as simulated by the MAPSS and BIOME3 biogeography models (ranges include both models).

	With CO_2 Effect		Without CO_2 Effect
Biome Type	FAR Scenarios	SAR Scenarios	SAR Scenarios
Tundra	67-80%	36-82%	32-70%
Taiga/Tundra	10-20%	20-28%	18-23%
Boreal Conifer Forests	74-98%	41-95%	14-63%
Temperate Evergreen Forests	78-87%	58-73%	29-66%
Temperate Mixed Forests	23-41%	33-47%	11-37%
Tropical Broadleaf Forests	60-89%	46-85%	32-76%
Savanna/Woodlands	80-84%	31-60%	51-59%
Shrub-Steppe	23-44%	15-45%	23-48%
Grasslands	38-41%	19-32%	17-40%
Arid Lands	7-24%	4-15%	3-15%

C.6.1. Control Climate

MAPSS and BIOME3 produce similar vegetation maps under current climate, but there are some differences. Some of the discrepancies between MAPSS and BIOME3 under current climate (Figure C-1) are due to questions of classification, especially in the drier types. For example, the Sahel region in Africa is labeled as 'shrub-steppe' in the original BIOME3 classification, but as various grassland types in MAPSS. The MAPSS grassland types do allow some shrubs, but the shrub density is usually reduced by the fire model, which assumes that there has been no reduction in fuel due to grazing. Were such land-use constraints included, the two models would be in better agreement on the classification. This classification difference between the models occurs over many of the drier parts of the world.

The models each appear to be better calibrated to their 'home' continents than either is to other continents. For example, MAPSS over-estimates the distribution of Temperate Evergreen Forests (conifers) in western Europe; while, BIOME3 overestimates the distribution of Temperate Mixed Forests (broadleaf) in western North America (Table C-1); yet, the two models are generally in agreement on the amount and location of temperate forests.

One area of significant departure from observed vegetation is the Pampas of southern South America. Both models simulate forests where grasslands are generally predominant. Various hypotheses for this discrepancy include unique soils, fire disturbance, rainfall seasonality and interannual variability of rainfall (VEMAP Members, 1995; Neilson, 1995; Neilson and Marks, 1994) and represent a focus for future research. Other local to regional errors in the MAPSS and BIOME3 classifications will be apparent to the knowledgeable reader. Reasons for these errors are many, but include 1) possible errors in the interpolated climate, 2) grazing, harvest, fire and other disturbances, and 3) missing or weak representation of some processes in the models. Globally, both models are reasonably accurate and are generally considered to be more accurate under altered climates than previous, empirical approaches (VEMAP Members, 1995). Empirical approaches cannot simultaneously simulate changes in vegetation distribution and changes in vegetation density and hydrology. Nor can they examine the sensitivity of the system to altered CO_2 concentrations. However, as the focus shifts to ever smaller regions or locales, the model uncertainty and the likelihood of error increases.

C.6.2. Future Vegetation Distribution

Both MAPSS and BIOME3 produce large shifts of cold-limited vegetation boundaries into higher latitudes and elevations. However, the water-controlled boundaries may exhibit any direction of change, depending on the interaction of several variables including among others, the relative changes in temperature and precipitation, and whether or not the direct effects of CO_2 have been incorporated.

The older GCM scenarios tend to be hotter than the newer ones and produce a more dramatic change in vegetation distribution. The MAPSS results under GFDL-R30 serve to illustrate one of the older simulations. MAPSS and BIOME2 (Haxeltine et al., 1996) were similar over the U.S. under this scenario (VEMAP Members, 1995), if both incorporated the direct CO_2 effects. MAPSS was far more xeric in response than BIOME2 without the direct CO_2 effects (ibid).

The Tundra decreases by as much as 1/3 to 2/3 of its present size, as does the Taiga/Tundra, under all scenarios and with both ecological models (Table C-1, Figures C-2, C-3, C-4 and C-5). The boreal forest expands in size under all scenarios ranging from 108% to 133% of its present size (MAPSS only). Since

BIOME3 includes the Taiga/Tundra, which contracts under all warming scenarios (MAPSS simulations), with the Boreal Conifer Forest, which expands under all scenarios (MAPSS simulations), the net change simulated by BIOME3 usually indicates a loss of Boreal Forest. However, the aggregation of the two types in BIOME3 hides the observation that the two vegetation types (as defined above) tend to change in opposite sign with respect to area, i.e., Taiga/Tundra decreasing, Boreal Conifer increasing. The two models are quite consistent in the simulated response of the combined biomes (Table C-1). Temperate forests (inclusive of both types) increase in area (107% to 158%). Tropical forests could either expand or contract, largely dependent on the inclusion of the direct CO_2 effect, but also dependent on the severity of the scenario. Savanna/woodlands expand or contract, depending on whether or not they are encroached upon by neighboring forests or semi-arid lands, again reflecting whether or not direct CO_2 effects are considered and on the scenario. BIOME3 shows a competitive displacement of tropical savannas by neighboring forests, due to the superior competitive ability in the model of the C_3 trees over the C_4 grasses under elevated CO_2. The total area of grasslands and shrublands in these simulations remains largely unchanged or expands by as much as 27%, depending on the CO_2 effect and the scenario. If the direct effects of CO_2 are included, arid lands tend to contract in all scenarios, shifting to less arid types (Table C-1, Figures C-2, C-3, C-4 and C-5). Without the direct CO_2, arid lands either expand or contract in area, depending on the climate scenario and the ecological model.

INTERGOVERNMENTAL PANEL
ON CLIMATE CHANGE
UNEP   WMO

C.6.3. Change in Vegetation Density (LAI)

Although temperature-controlled vegetation boundaries shift predictably in all cases, water-controlled boundaries could shift any direction, reflecting either more or less beneficial water status. Likewise, vegetation change does not simply consist of shifts in the boundaries between homogeneous blocks of vegetation. Indeed, changes in vegetation density (via leaf area index, LAI) may often be more informative, since changes in LAI in water-limited areas generally indicate a change in the site water status and carrying capacity (Tables C-2, C-3; Figures C-6, C-7, C-8 and C-9). The change in LAI could also be taken as an indication of what could happen in the near term, since changes in LAI can occur in a matter of a few years while adjustments of vegetation structure and composition take much longer.
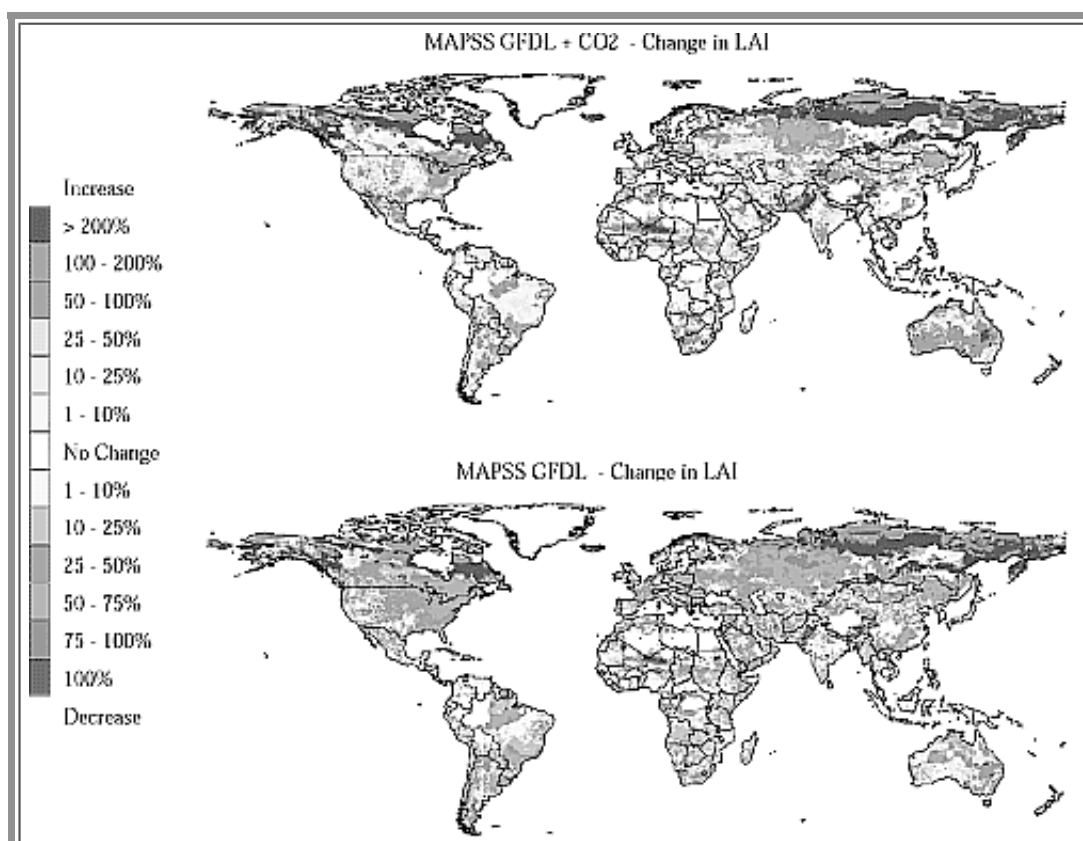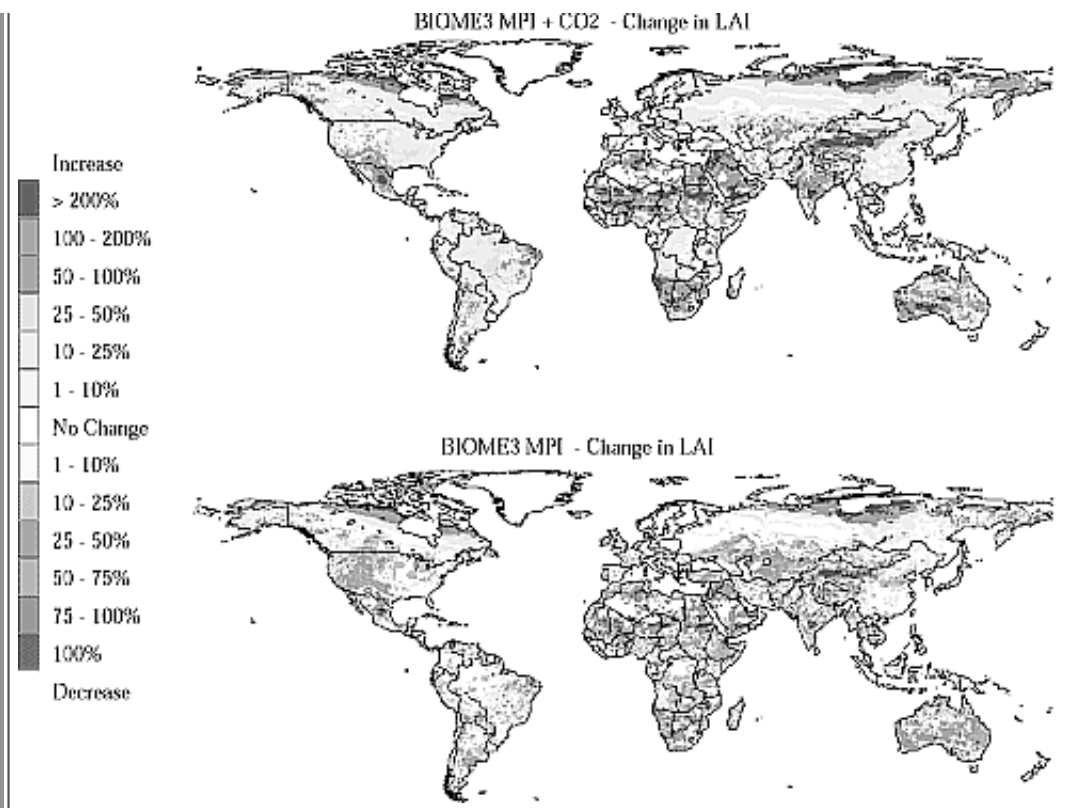

Figure C-6: The potential change in vegetation leaf area index (LAI), which can be considered as an index of vegetation density or biomass, as simulated under the GFDL-R30 2 x CO_2 GCM experiment (Geophysical Fluid Dynamics Laboratory, slab ocean, no sulfate aerosols), by MAPSS, both (a) with and (b) without a direct, physiological CO_2 effect.

Figure C-7: The potential change in vegetation leaf area index (LAI), which can be considered as an index of vegetation density or biomass, as simulated under the MPI-T106 GCM experiment (Max Planck Institute, 2 x CO_2 greenhouse gas radiative forcing, extracted from transient simulation, no sulfate aerosols), by BIOME3, both (a) with and (b) without a direct, physiological CO_2 effect.
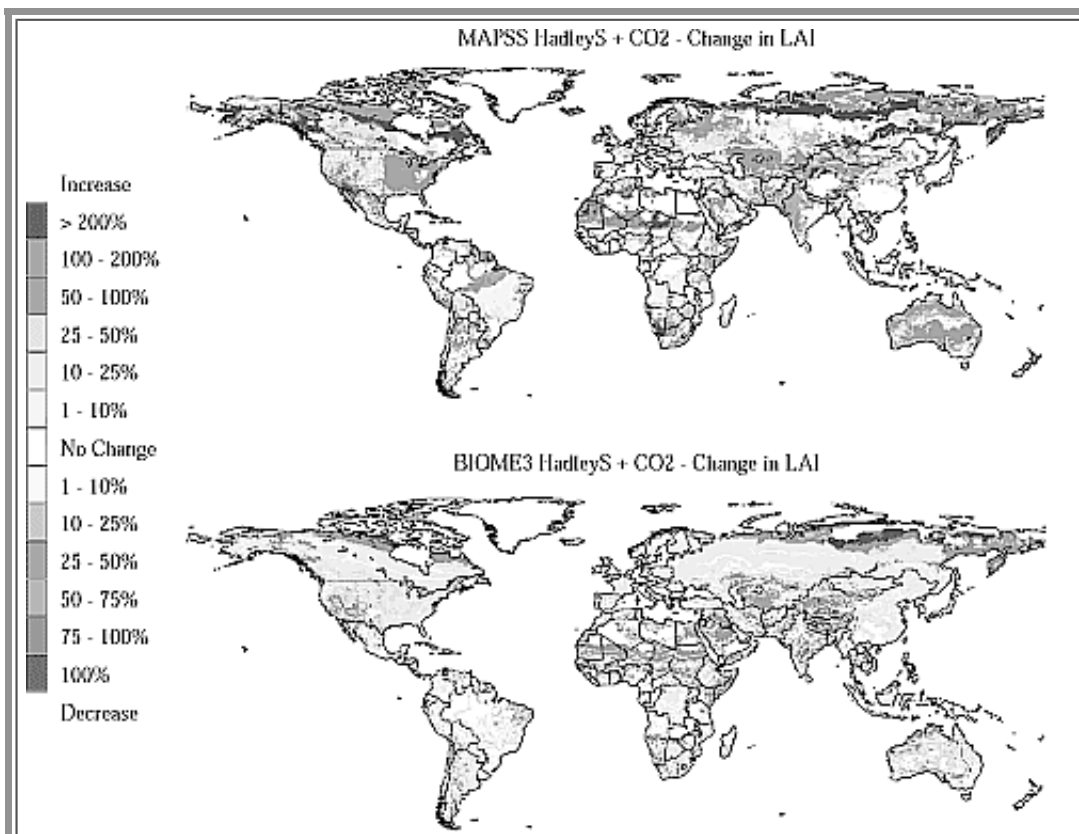

Figure C-8: The potential change in vegetation leaf area index (LAI),

which can be considered as an index of vegetation density or biomass, as simulated under the HADCM2SUL GCM experiment (Hadley Center, 2 x CO_2 greenhouse gas radiative forcing, extracted from transient simulation, plus sulfate aerosols), by (a) MAPSS and (b) BIOME3. Both models have incorporated a direct, physiological CO_2 effect. This figure is a companion to Figure C-4.
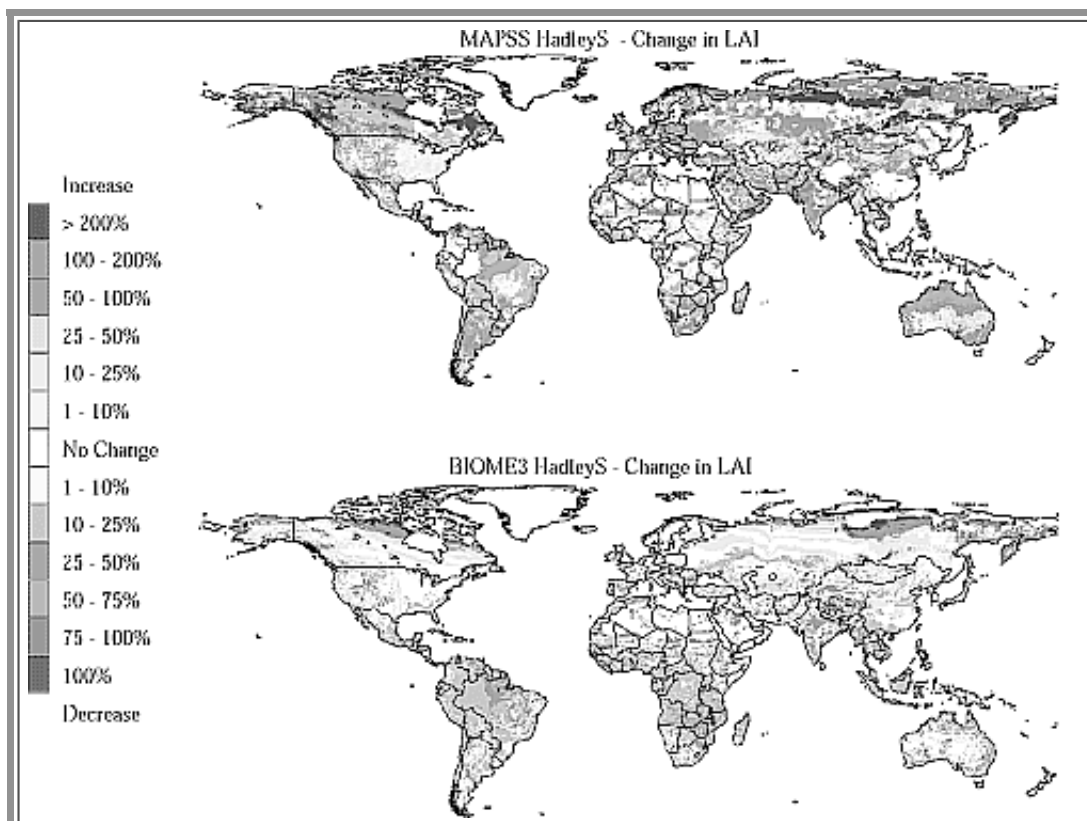

Figure C-9: The potential change in vegetation leaf area index (LAI), which can be considered as an index of vegetation density or biomass, as simulated under the HADCM2SUL GCM experiment (Hadley Center, 2 x CO_2 greenhouse gas radiative forcing, extracted from transient simulation, plus sulfate aerosols), by (a) MAPSS and (b) BIOME3. A direct, physiological CO_2 effect is not incorporated in either model. This figure is a companion to Figure C-5.

MAPSS and BIOME3 produce generally similar maps of change in LAI when forced by the same scenario, except that MAPSS produces a consistently stronger drought effect (compare Figures C-6 and C-7 and Figures C-8 and C-9). For example, within the U.S., when not including a direct CO_2 effect (Figure C-9), both models indicate increases in LAI in the SouthWest and either an increase or no change in LAI over most of the eastern U.S. Both models simulate a decline or no change (BIOME3) over much of the western U.S. (excluding the SW). Both models produce increases in LAI over parts of the Sahara/Sahel, either with or without the direct CO_2 effect under all scenarios, both old and new.

Likewise, both models under all scenarios indicate some increases in LAI over much of the arid interior of Australia. In general, there appear to be increases in LAI in already low LAI regions, either arid or cold. The increases in cold regions are due to expansion of forests into non-forested areas. The increases in arid areas are due to increased rainfall, a consequence of a generally more vigorous hydrologic cycle. There are many other consistencies between the two biogeography models with respect to the relative

regional or subregional simulated LAI changes. A more complete discussion of simulated LAI patterns from the VEMAP models over the conterminous U.S. is in preparation.

(continues on next page...)

INTERGOVERNMENTAL PANEL
ON CLIMATE CHANGE

UNEP   WMO

(continued...)

If the direct effects of CO_2 are minimal and the future scenarios are relatively warm, decreases in LAI could occur over very large forested areas, ranging up to nearly 2/3 or more of the areas of boreal, temperate and tropical forests (Table C-2). By contrast, if the direct effects of CO_2 are strong and scenarios are not too warm, then all forest vegetation zones could experience increased biomass over as much as 2/3 or more of their areas (Table C-3). More likely, the responses will be intermediate with large regional contrasts, decreases in vegetation density in some areas, increases in others. Even though these are equilibrium simulations, a simulated decline in LAI generally implies a less favorable water balance and a loss of vegetation density. These losses imply a process of loss over some time period. We can only draw inferences about how rapidly such losses would occur, based on the simulated amount of loss. The regions that could experience declining LAI (Figure C-6, Figure C-7, Figure C-8 and Figure C-9), would exhibit spatial gradients in response from mild decline grading into potentially catastrophic dieback. All reaches along the decline gradients would experience drought stress, which could trigger other responses, such as pest infestations and fire. Following disturbance by drought, infestation or pests, new vegetation, either of the same or of a different type would grow, but to a lower density.

Including both equilibrium and 'transient' scenarios, MAPSS was run under four different scenarios (not counting the sulfate scenario, HADSUL). These range in global temperature increase (delta T) at the time of 2 x CO_2 from 1.7 (HADGHG) to 5.2°C (UKMO) (Annex B). In general, the areas of forest decline within individual biomes (incorporating a direct CO_2 effect) increase linearly with increasing delta T in the temperate and boreal forests; while, the areas of increased forest density decrease with increasing delta T. Tropical forests exhibit a similar pattern across the three FAR scenarios, but under the cooler HADGHG scenario show a large decline as simulated by MAPSS. By contrast, BIOME3, under the HADGHG scenario, shows almost no change in tropical forest density. Interestingly, adjacent tropical savannas increase in density in both ecological models under the HADGHG scenario.

C.6.4. Equilibrium vs. "Transient" Scenarios and the Importance of Elevated CO_2

The newer climate scenarios (IPCC 1996, WG I, Section 6), extracted from transient GCM simulations, are as a group quite different from the older, equilibrium scenarios (IPCC 1990, WG I, Section 3), in terms of the simulated ecological responses that these scenarios produce. All of the older scenarios produce large regions showing LAI declines (especially in temperate to high latitudes), as well as gains, even when the direct effects of CO_2 are included (MAPSS simulations, Figure C-6, OSU and UKMO scenarios not shown). By contrast, under the newer scenarios, if a direct CO_2 effect is assumed, then there are very few regions with declines in LAI, as simulated by both MAPSS and BIOME3 (Figures C-7, C-8); rather, most of the world is simulated with an increased LAI. Actual increases in LAI could be limited by nitrogen availability in some areas, although elevated soil temperatures could increase decomposition, releasing more nitrogen (McGuire et al., 1995; VEMAP Members, 1995). The first-order differences between the older and newer scenarios are likely due to the smaller global temperature increases in the newer climate scenarios, which came from GCMs that had not attained their full equilibrium temperature changes.

C.6.5. Sulfate Aerosols

The incorporation of sulfate aerosols produced a cooling effect in the HADCM2SUL run compared to

the HADCM2GHG run, which lacked the sulfate forcing (GHG runs are not shown). The vegetation response to the sulfate forcing is observable in the model output from both MAPSS and BIOME3, but is relatively small compared to the differences between the newer and older climate scenarios. The newer scenarios produce widespread enhanced vegetation growth, even without the sulfate effect, if direct CO_2 effects are included and widespread decline if the CO_2 effects are excluded. The presence of the sulfate-induced cooling produces a much smaller amplitude effect on the vegetation than does the presence or absence of the direct effects of elevated CO_2 on water-use-efficiency.

C.6.6. Change in Annual Runoff

Changes in annual runoff (Figure C-10) were mapped for all scenarios from both MAPSS and BIOME3. The changes in runoff are more stable among the different climate scenarios than are the simulated changes in LAI. The relative stability of simulated runoff change may reflect that runoff is a passive drainage process; whereas, evapotranspiration is a biological process and a function of the product of LAI and stomatal conductance. If stomatal conductance is reduced, e.g., via a direct CO_2 effect, LAI will compensate by increasing and runoff will show little change (Neilson and Marks, 1994). Some of the obvious differences between MAPSS and BIOME3 can be attributed to structural differences in the models. BIOME3 calculates water balance daily, even though all inputs are monthly; whereas, MAPSS calculates water balance monthly. This difference alone could be causing the more extreme responsiveness of MAPSS, which shows both larger runoff increases and larger losses in different regions. On the other hand, MAPSS uses a 3-layer soil with roots only in the top two layers; while BIOME3 uses a 2-layer soil with roots in both layers. The third layer in MAPSS provides a consistent base flow and might explain why MAPSS produces runoff in some drier regions, such as the western U.S., while BIOME3 does not. The hydrology models in both MAPSS and BIOME3, although process-based, are considered prototypes for eventual replacement by more elaborate models (see for example, the PILPS model intercomparison study; Love and Henderson-Sellers, 1994).
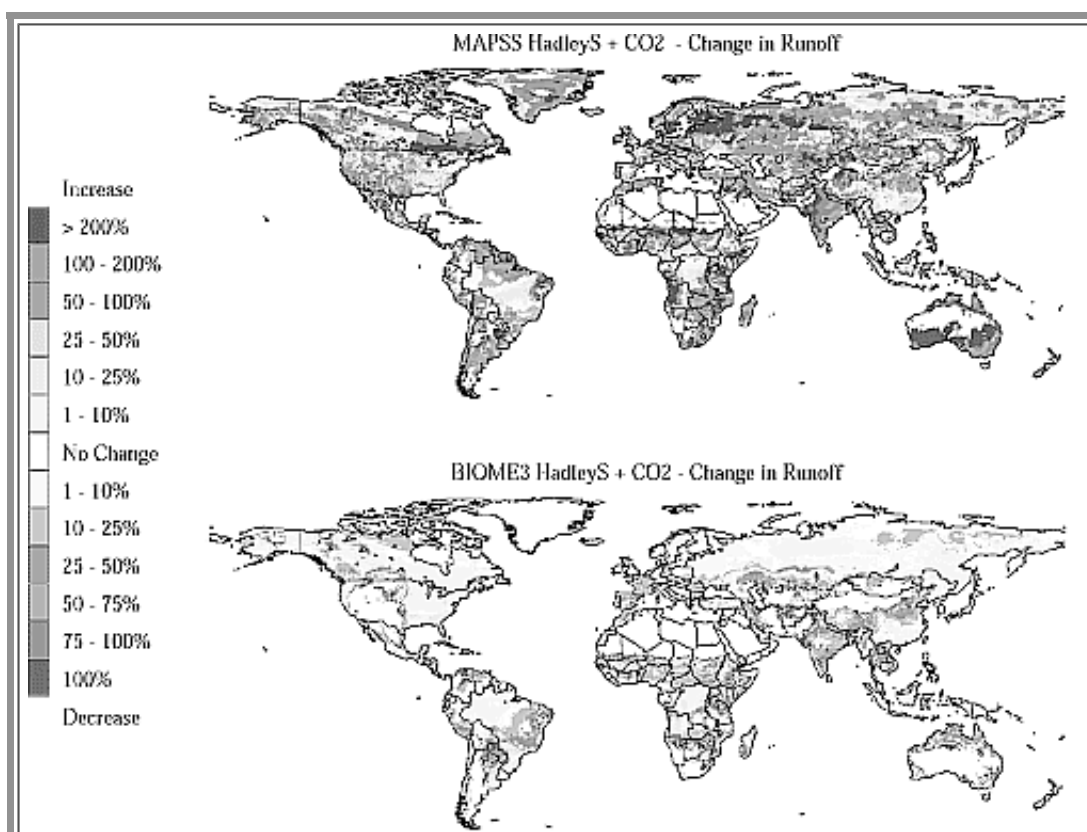

Figure C-10: The potential change in annual runoff, as simulated under the HADCM2SUL GCM experiment (Hadley Center, 2 x CO_2 greenhouse gas

radiative forcing, extracted from transient simulation, plus sulfate aerosols), by (a) MAPSS and (b) BIOME3. Both models have incorporated a direct, physiological CO_2 effect. This figure is a companion to Figures C-4 and C-8.

In general, MAPSS and BIOME3 produce similar regional patterns in the estimated changes in runoff. Although the magnitude of the changes are different, there are broad similarities in the sign of the change (but, clearly not in all regions). The largest area of regional difference between the two models is in interior Eurasia (Figure C-10).

Runoff generally increases in the Tundra, due to higher temperatures, more precipitation and more melting (Tables C-4, C-5). It decreases in the Taiga/Tundra due to encroachment of high-density boreal forest into low density vegetation (hence, higher transpiration). Runoff results are varied in the temperate forests, but Temperate Mixed forests tend to present a higher likelihood of reduced runoff over large areas (range 51% to 88% of the area under all scenarios) than of increased runoff (range 11% to 47% of the area under all scenarios, Tables C-4, C-5). Even the most benign scenarios indicate a minimum of 51% of the area of the world's temperate evergreen forests could experience a runoff decline; whereas, a maximum of 47% of the area would experience increased runoff. Temperate Evergreen Forests exhibit a greater likelihood of increased runoff over large areas (range 29% to 87% of the area under all scenarios) than decreased runoff (range 11% to 68%), but the overlap in these increase and decrease ranges indicates the degree of uncertainty in the simulations. However, much of the increased runoff in the Temperate Evergreen forested areas is due to increased winter runoff, which is not necessarily available for use by ecosystems, irrigation or domestic purposes. Runoff from tropical forest areas could either increase or decrease over large areas, depending largely on the importance of the direct CO_2 effects.

Runoff from drier vegetation types is regionally variable and exhibits both increases and decreases, depending on the direct CO_2 effects and regional rainfall patterns.

INTERGOVERNMENTAL PANEL
ON CLIMATE CHANGE
UNEP   WMO

C.7. Conclusions

MAPSS and BIOME3 produce qualitatively similar results under alternative future climate scenarios, with or without including a direct, physiological CO_2 effect. However, MAPSS produces consistently stronger drought effects with increasing temperature than does BIOME3. When under common scenarios, the two models produce similar subregional sensitivities. That is, if two adjacent subregions show opposite sign responses under a future climate in MAPSS, they will tend to exhibit the same relationship in BIOME3, but the overall sensitivity will be lower in BIOME3. The newer scenarios, constructed from transient GCM experiments, are consistently less xeric, as measured by simulated changes in leaf area index (LAI), than the older, equilibrium GCM scenarios. Under the newer scenarios, both ecological models indicate an overall increase in LAI (although nutrient constraints could limit or delay the increase), when a direct physiological CO_2 effect is included. However, if the direct CO_2 effects are not included, both models indicate a general reduction in global vegetation density.

The changes in vegetation leaf area (LAI) simulated by both MAPSS and BIOME3 are analogous to the changes in soil water content reported by earlier GCM experiments (IPCC 1996, WG I, Section 6). Those earlier experiments maintained a fixed vegetated land surface. That is, the vegetation type and density were not allowed to respond to changes in either climate or elevated CO_2 concentration. Therefore, as evaporative demand went up in those simulations, soil water content decreased, or was totally depleted. MAPSS and BIOME3, however, absorb those processes directly in the vegetation response. Both models simulate water-limited LAI by maximizing the LAI that can be supported and just barely transpire available soil water. Thus, in the equilibrium solution to LAI, soil water is fully utilized and can't change much under altered climates. Changes in the site water balance are, therefore, indicated by changes in LAI.

The newer climate scenarios used in this analysis are relatively cool in comparison to other possible new scenarios (IPCC 1996, WG I, Section 6). Therefore, the analyses presented here must be considered as a relatively conservative subset of the possible future ecological responses.

Although many of the simulations from both MAPSS and BIOME3 indicate potentially large expansions of tropical and in some cases temperate forests, actual expansions would be limited by urban and agricultural land-use constraints, unsuitable soils in some areas and slow dispersal rates, among other factors. Even so, if a forest is anticipated to expand into a region formerly indicated as shrubland, any agriculture in the region might expect an increase in potential productivity, and vice versa. Such changes between forest and shrubland are usually underlain by a change in LAI, which reflects the site water balance. An increase or decrease in LAI indicates a change in the water or energy balance and the potential biomass density or carrying capacity that could be supported on the site, regardless of whether the biomass is 'natural' or agricultural (dryland agriculture only).

The results presented here are for steady-state, or equilibrium conditions and do not directly indicate how the systems would behave in their transient responses toward a new equilibrium. For example, in areas where LAI is indicated to decline, it may be that equilibrium runoff is indicated to increase. However, one hypothesis is that during the processes of LAI decline, increased evaporative demand could cause reductions in runoff, before the vegetation becomes sufficiently drought-stressed for the LAI to be reduced. After further time, if the vegetation is sufficiently drought stressed, a rapid dieback could occur and might be facilitated by pests and fire. Were vegetation to undergo such a large dieback, then transpiration demand would be temporarily reduced and runoff could increase substantially. Thus, before a new equilibrium is attained with new vegetation growth, streams could go through a dry to wet

oscillation. These possible hydrologic responses to vegetation change are, however, of a different timeframe (years) than possible short term floods and droughts that could occur simply due to increased variation of extreme weather events (IPCC 1996, WG I, Section 6).

At least two contrasting, transient trajectories of vegetation change are possible. If a large, direct CO_2 benefit were to occur, vegetation could increase in growth and biomass under relatively cool, early warming conditions, only to experience drought-stress and decline or dieback under the hotter, later stages of warming. Alternatively, if direct CO_2 benefits are more muted, vegetation could become drought-stressed and experience decline or dieback within the next few decades even under mild warming. Expansion of forests into cooler zones would likely lag behind decline and dieback in warmer zones, producing a transient reduction in forest area, possible increases in pests and fire, and possibly large releases of CO_2 to the atmosphere (King and Neilson, 1992; Smith and Shugart, 1993).

INTERGOVERNMENTAL PANEL
ON CLIMATE CHANGE
UNEP   WMO

References

Bazzaz, F.A. 1990:

The Response of Natural Ecosystems to the Rising Global CO_2 Levels. Annual Review of Ecology and Systematics, 21, 167-196.

Bazzaz, F.A., S.L. Bassow, G.M. Berntson, and S.C. Thomas, 1996:

Elevated CO_2 and terrestrial vegetation: implications for and beyond the global carbon budget. In: Global Change and Terrestrial Ecosystems [Walker, B. and W. Steffen (eds.)]. Cambridge University Press, Cambridge, pp. 43-76.

Bengtsson, L., M. Botzet, and M. Esch, 1995:

Hurricane-type vortices in a general circulation model. Tellus, 47A, 1751-1796.

Bengtsson, L., M. Botzet, and M. Esch, 1996:

Will greenhouse gas-induced warming over the next 50 years lead to higher frequency and greater intensity of hurricanes? Tellus, 48A, 57-73.

Curtis, P.S. 1996:

A meta-analysis of leaf gas exchange and nitrogen in trees grown under elevated carbon dioxide. Plant, Cell and Environment, 19, 127-137.

Curtis, P.S., C.S. Vogel, K.S. Pregitzer, D.R. Zak, and J.A. Teeri, 1995:

Interacting effects of soil fertility and atmospheric CO_2 on leaf area growth and carbon gain physiology in Populus X euramericana (Dode) Guinier. New Phytologist, 129, 253-263.

Eamus, D., 1991:

The interaction of rising CO_2 and temperatures with water use efficiency. Plant, Cell and Environment, 14, 843-852.

Eamus, D., 1996a:

Responses of field grown trees to CO_2 enrichment. Commonwealth Forestry Review, 75, 39-47.

Eamus, D. 1996b:

Tree responses to CO_2 enrichment: CO_2 and temperature interactions, biomass allocation and stand-scale modeling. Tree Physiology, 16, 43-47.

Grulke, N.E., J.L. Hom, and S.W. Roberts, 1993:

Physiological adjustment of two full-sib families of ponderosa pine to elevated CO_2. Tree Physiology, 12, 391-401.

Grulke, N.E., G.H. Riechers, W.C. Oechel, U. Hjelm, and C. Jaeger. 1990:

Carbon balance in tussock tundra under ambient and elevated atmospheric CO_2. Oecologia, 83, 485-494.

Haxeltine, A. and I.C. Prentice, 1996: BIOME3:

An equilibrium terrestrial biosphere model based on ecophysiological constraints, resource availability and competition among plant functional types. Global Biogeochemical Cycles, 10(4), 693-710.

Haxeltine, A., I.C. Prentice, and I.D. Creswell, 1996:

A coupled carbon and water flux model to predict vegetation structure. Journal of Vegetation Science, 7(5), 651-666.

Hunt, E.R. and S.W. Running, 1992:

Simulated dry matter yields for aspen and spruce stands in the North American boreal forest. Canadian Journal of Remote Sensing, 18, 126-133.

IPCC, 1990:

Climate Change: The IPCC Scientific Assessment [Houghton, J.T., G.J. Jenkins, and J.J. Ephraums (eds.)]. Cambridge University Press, Cambridge and New York, 365 pp.

Cubasch, U. and R.D. Cess, Chapter 3. Processes and Modelling, pp. 69-91.

Mitchell, J.F.B., S. Manabe, V. Meleshko, and T. Tokioka, Chapter 5. Equilibrium Climate Change — and its Implications for the Future, pp. 131-172.

IPCC, 1996:

Climate Change 1995: The Science of Climate Change. Contribution of Working Group I to the Second Assessment Report of the Intergovernmental Panel on Climate Change [Houghton, J.T., L.G. Meira Filho, B.A. Callander, N. Harris, A. Kattenberg, and K. Maskell (eds.)]. Cambridge University Press, Cambridge and New York, 572 pp.

Gates, W.L., A. Henderson-Sellers, G.J. Boer, C.K. Folland, A.Kitoh, B.J. McAvaney, F. Semazzi, N. Smith, A.J. Weaver, and Q.-C. Zeng, Chapter 5. Climate Models — Evaluation, pp. 235-284.

Kattenberg, A., F. Giorgi, H. Grassl, G.A. Meehl, J.F.B. Mitchell, R.J. Stouffer, T. Tokioka, A. J. Weaver, and T.M.L. Wigley, Chapter 6. Climate Models — Projections of Future Climate, pp. 289-357.

IPCC, 1996. Climate Change 1995:

Impacts, Adaptations and Mitigation of Climate Change: Scientific-Technical Analyses. Contribution of Working Group II of the Second Assessment Report of the Intergovernmental Panel on Climate Change [Watson, R.T., M.C. Zinyowera, and R.H. Moss (eds.)]. Cambridge University Press, Cambridge and New York, 880 pp.

Kirschbaum, M.U.F., Chapter A. Ecophysiological, Ecological, and Soil Processes in Terrestrial Ecosystems: A Primer on General Concepts and Relationships, pp. 57-74.

Kirschbaum, M.U.F. and A. Fischlin, Chapter 1. Climate Change Impacts on Forests, pp. 95-129.

Johns, T.C., R.E. Carnell, J.F. Crossley, J.M. Gregory, J.F.B. Mitchell, C.A. Senior, S.F.B. Tett, and R.A. Wood, 1997:

The second Hadley Centre coupled ocean-atmosphere GCM: Model description, spinup and validation. Climate Dynamics (submitted).

Kirschbaum, M.U.F., D.A. King, H.N. Comins, R.E. McMurtrie, B.E. Medlyn, S. Pongracic, D. Murty, H. Keith, R.J. Raison, P.K. Khanna, and D.W. Sheriff. 1994:

Modelling forest response to increasing CO_2 concentration under nutrient-limited conditions. Plant, Cell and Environment, 17, 1081-1099.

King, G.A. and R.P. Neilson, 1992:

The transient response of vegetation to climate change: A potential source of CO_2 to the atmosphere. Water, Air, Soil Pollution, 64, 365-383.

Körner, C. 1995. Towards a better experimental basis for upscaling plant responses to elevated CO_2 and climate warming. Plant, Cell and Environment, 18, 1101-1110.

Leemans, R. and W.P. Cramer, 1991:

The IIASA database for mean monthly values of temperature, precipitation, and cloudiness on the global terrestrial grid. International Institute for Applied Systems Analysis RR-91-18, pp. 1-62.

Love, P.K. and A. Henderson-Sellers, 1994:

Land-surface climatologies of AMIP-PILPS models and identification of regions for future investigation (PILPS Phase 3a). IGPO Publication Series 13, pp. 1-48.

McGuire, A.D., J.M. Melillo, and L.A. Joyce, 1995:

The role of nitrogen in the response of forest net primary production to elevated atmospheric carbon dioxide. Annual Review of Ecology and Systematics, 26, 473-503.

McGuire, A.D., J.M. Melillo, L.A. Joyce, D.W. Kicklighter, A.L. Grace, B. Moore, and C.J. Vorosmarty, 1992:

Interactions between carbon and nitrogen dynamics in estimating net primary productivity for potential vegetation in North America. Global Biogeochemical Cycles, 6, 101-124.

Melillo, J.M., A.D. McGuire, D.W. Kicklighter, B. Moore, C.J. Vorosmarty, and A.L. Schloss, 1993:

Global climate change and terrestrial net primary production. Nature, 363, 234-240.

Mitchell, J.F.B., T.C. Johns, J.M. Gregory, and S. Tett, 1995:

Climate response to increasing levels of greenhouse gases and sulphate aerosols. Nature,

376, 501-504.

Mitchell, J.F.B. and D. A. Warrilow, 1987:

Summer dryness in northern mid latitudes due to increased CO_2. Nature, 330, 238-240.

Neilson, R.P., 1995:

A model for predicting continental-scale vegetation distribution and water balance. Ecological Applications, 5, 362-385.

Neilson, R.P. and D. Marks, 1994:

A global perspective of regional vegetation and hydrologic sensitivities from climatic change. Journal of Vegetation Science, 5, 715-730.

Neilson, R.P. and S.W. Running, 1996:

Global dynamic vegetation modelling: coupling biogeochemistry and biogeography models. In: Global Change and Terrestrial Ecosystems [Walker, B. and W. Steffen (eds.)]. Cambridge University Press, Cambridge, pp. 451-465.

Norby, R.J. 1996:

Forest canopy productivity index. Nature, 381, 564.

Parton, W.J., D.S. Schimel, C.V. Cole, and D. Ojima, 1987:

Analysis of factors controlling soil organic levels of grasslands in the Great Plains. Soil Science Society of America, 51, 1173-1179.

Parton, W.J., J.M.O. Scurlock, D.S. Ojima, T.G. Gilmanov, R.J. Scholes, D.S. Schimel, T. Kirchner, J.-C. Menaut, T. Seastedt, E.G. Moya, A. Kamnalrut, and J.I. Kinyamario, 1993:

Observations and modeling of biomass and soil organic matter dynamics for the grassland biome worldwide. Global Biogeochemical Cycles, 7, 785-809.

Parton, W.J., J.W.B. Stewart, and C.V. Cole, 1988:

Dynamics of C, N, P and S in grassland soils: a model. Biogeochemistry, 5, 109-131.

Prentice, I.C., W. Cramer, S.P. Harrison, R. Leemans, R.A. Monserud, and A.M. Solomon, 1992:

A global biome model based on plant physiology and dominance, soil properties and climate. Journal of Biogeography, 19, 117-134.

Raich, J.W., E.B. Rastetter, J.M. Melillo, D.W. Kicklighter, P.A. Steudler, B.J. Peterson, A.L. Grace, B. Moore, and C.J. Vorosmarty, 1991:

Potential net primary productivity in South America: Application of a global model. Ecological Applications, 1, 399-429.

Running, S.W. and E.R. Hunt, 1993:

Generalization of a forest ecosystem process model for other biomes, BIOME-BGC, and an application for global-scale models. In: Scaling Physiological Processes: Leaf to Globe

[Ehleringer, J.R. and C.B. Field (eds.)]. Academic Press, Inc., San Diego, CA, p. 141-158.

Schlesinger, M.E. and Z.C. Zhao, 1989:

Seasonal climatic change introduced by double CO_2 as simulated by the OSU atmospheric GCM/mixed-layer ocean model. Journal of Climate, 2, 429-495.

Shugart, H.H. and T.M. Smith, 1996:

A review of forest patch models and their application to global change research. Climatic Change, 34(2), 131-153.

Smith, T.M. and H.H. Shugart, 1993:

The transient response of terrestrial carbon storage to a perturbed climate. Nature, 361, 523-526.

Teskey, R.O. 1997:

Combined effects of elevated CO_2 and air temperature on carbon assimilation of Pinus taeda trees. Plant, Cell and Environment, 20, 373-380.

VEMAP Members, 1995:

Vegetation/ecosystem modeling and analysis project: Comparing biogeography and biogeochemistry models in a continental-scale study of terrestrial ecosystem responses to climate change and CO_2 doubling. Global Biogeochemical Cycles, 9, 407-437.

Woodward, F.I. and T.M. Smith, 1994:

Predictions and measurements of the maximum photosynthetic rate at the global scale. In: Ecophysiology of Photosynthesis [Schulze, E.-D. and M.M. Caldwell (eds.)]. Ecological Studies, vol. 100. Springer-Verlag, New York, pp. 491-509.

Woodward, F.I., T.M. Smith and W.R. Emanuel, 1995:

A global land primary productivity and phytogeography model. Global Biogeochemical Cycles, 9, 471-490.

Wullschleger, S.D., W.M. Post, and A.W. King. 1995:

On the Potential for a CO_2 Fertilization Effect in Forest Trees: An Assessment of 58 Controlled-Exposure Studies and Estimates of the Biotic Growth Factor. In: Biotic Feedbacks in the Global Climate System [Woodwell, G.M. and F.T. Mackenzie (eds.)]. Oxford University Press, New York, pp. 85-107.
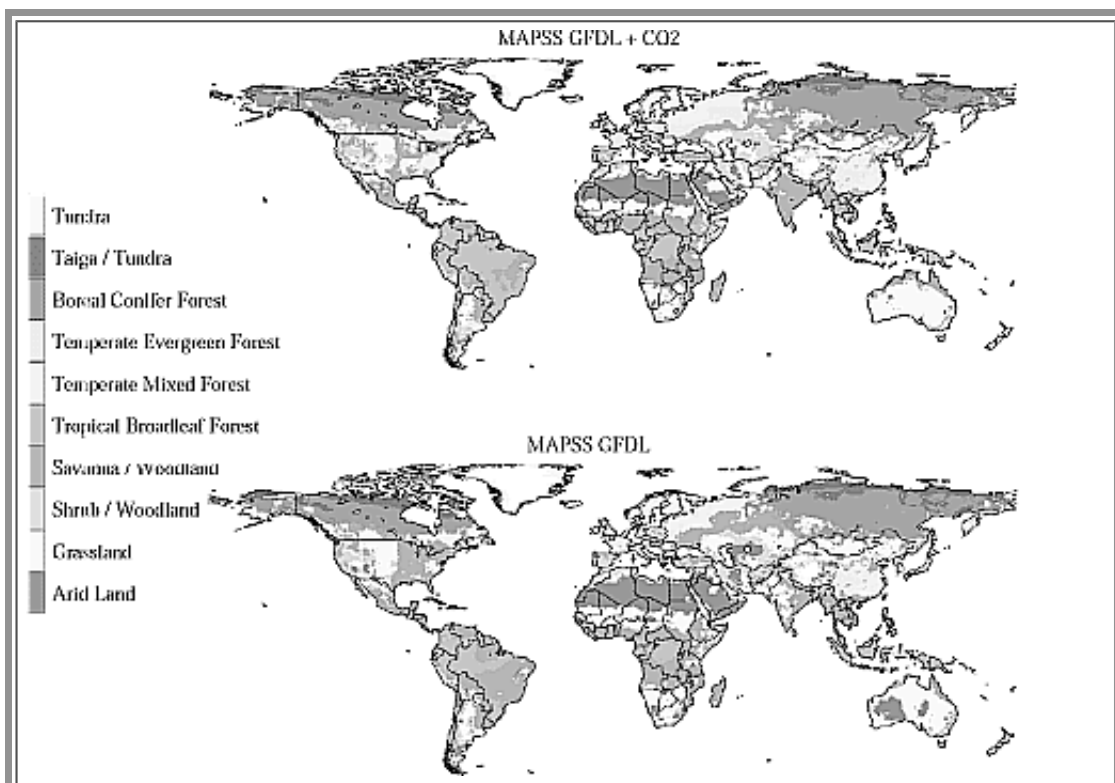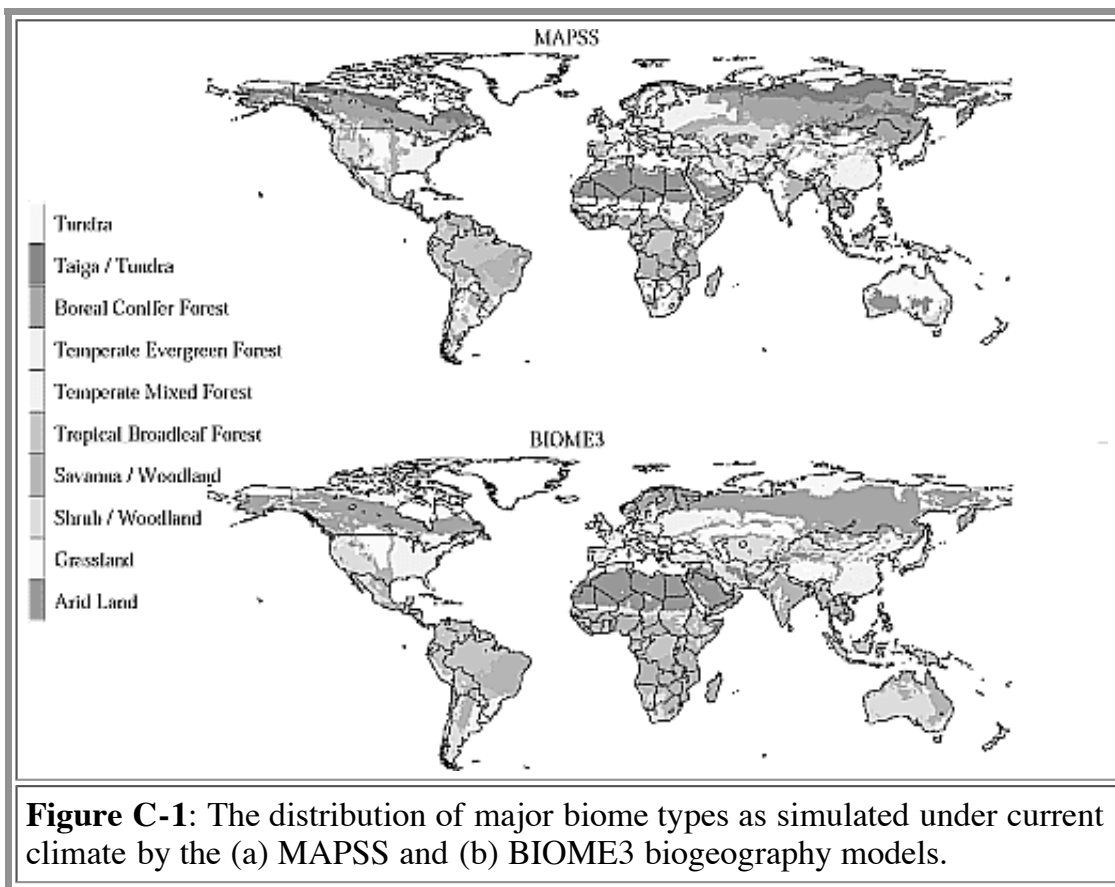
Figure C-1: The distribution of major biome types as simulated under current climate by the (a) MAPSS and (b) BIOME3 biogeography models.

Figure C-2: The potential distribution of major biomes as simulated under the GFDL-R30 2 x CO_2 GCM experiment (Geophysical Fluid Dynamics Laboratory, slab ocean, no sulfate aerosols), by MAPSS, both (a) with and (b) without a direct, physiological CO_2 effect.
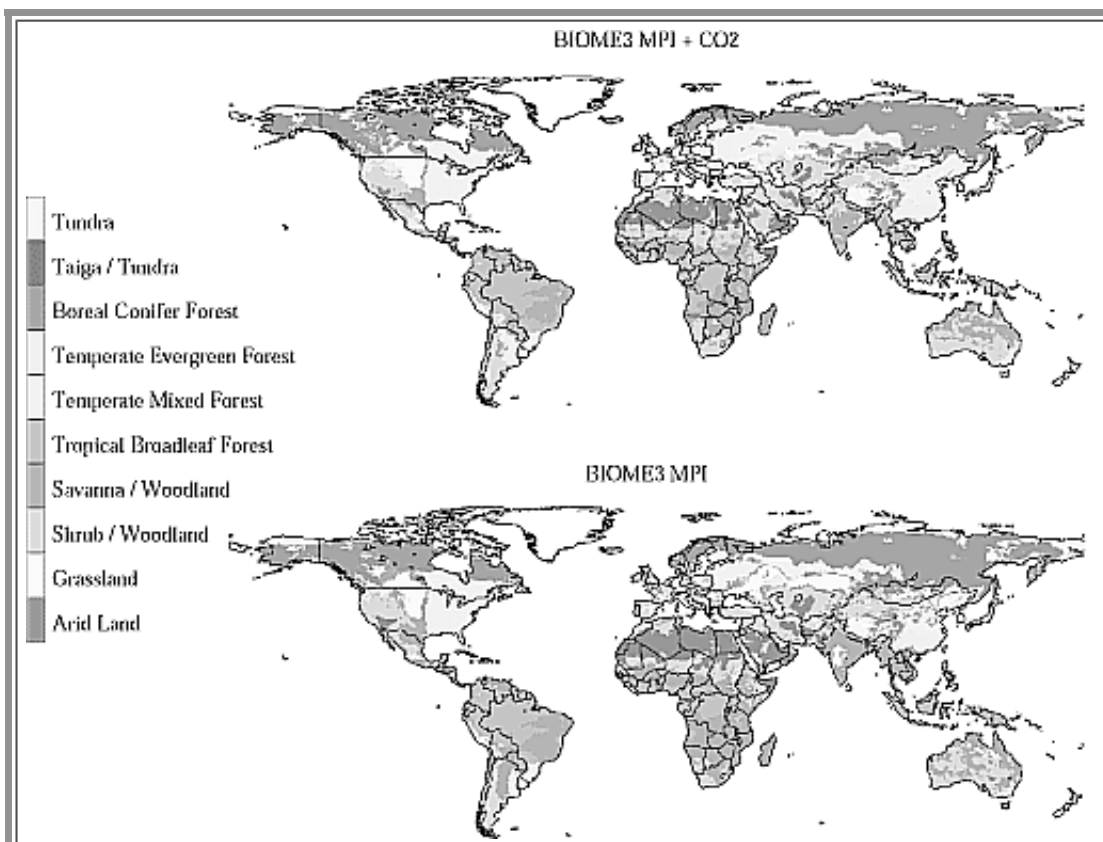
BIOME3 MPI + CO2

Tundra
Taiga / Tundra
Boreal Conifer Forest
Temperate Evergreen Forest
Temperate Mixed Forest
Tropical Broadleaf Forest
Savanna / Woodland
Shrub / Woodland
Grassland
Arid Land

BIOME3 MPI

Figure C-3: The potential distribution of major biomes as simulated under the MPI-T106 GCM experiment (Max Planck Institute, 2 x CO_2 greenhouse gas radiative forcing, extracted from transient simulation, no sulfate aerosols), by BIOME3, both (a) with and (b) without a direct, physiological CO_2 effect.
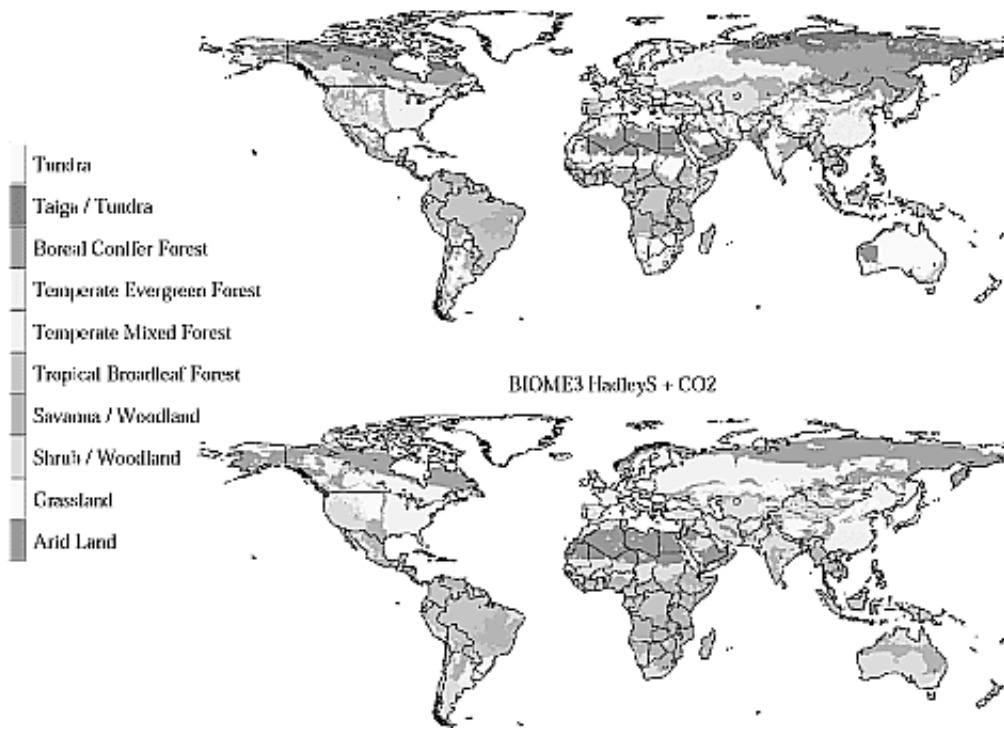
MAPSS HadleyS + CO2

BIOME3 HadleyS + CO2

Tundra
Taiga / Tundra
Boreal Conifer Forest
Temperate Evergreen Forest
Temperate Mixed Forest
Tropical Broadleaf Forest
Savanna / Woodland
Shrub / Woodland
Grassland
Arid Land

Figure C-4: The potential distribution of major biomes as simulated under the HADCM2SUL GCM experiment (Hadley Center, 2 x CO_2 greenhouse gas radiative forcing, extracted from transient simulation, plus sulfate aerosols), by (a) MAPSS and (b) BIOME3. Both models have incorporated a direct, physiological CO_2 effect.
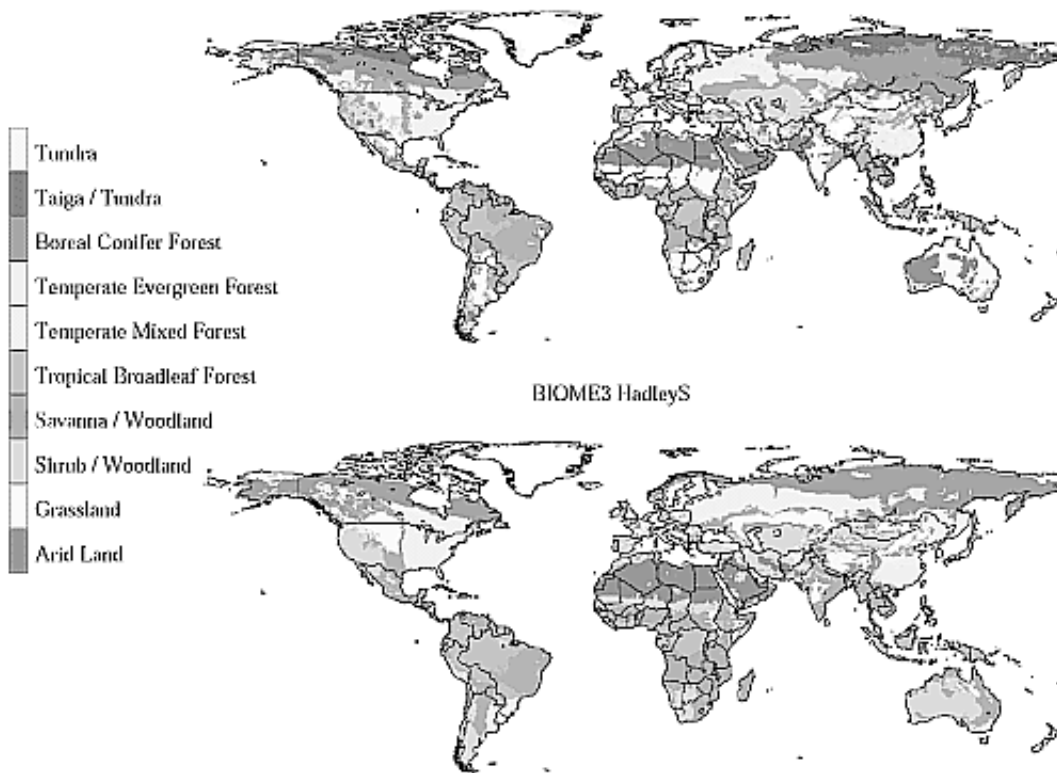

MAPSS HadleyS

BIOME3 HadleyS

Tundra
Taiga / Tundra
Boreal Conifer Forest
Temperate Evergreen Forest
Temperate Mixed Forest
Tropical Broadleaf Forest
Savanna / Woodland
Shrub / Woodland
Grassland
Arid Land

Figure C-5: The potential distribution of major biomes as simulated under the HADCM2SUL GCM experiment (Hadley Center, 2 x CO_2 greenhouse gas

radiative forcing, extracted from transient simulation, plus sulfate aerosols), by (a) MAPSS and (b) BIOME3. A direct, physiological CO_2 effect is not incorporated in either model.

INTERGOVERNMENTAL PANEL
ON CLIMATE CHANGE

UNEP   WMO